

# Dielectrophoresis of Surface Conductance Modulated Single-Walled Carbon Nanotubes Using Catanionic Surfactants

Youngjin Kim,<sup>†</sup> Seunghyun Hong,<sup>†</sup> Sehun Jung,<sup>†</sup> Michael S. Strano,<sup>‡</sup> Jaeboong Choi,<sup>†</sup> and Seunghyun Baik<sup>\*,†</sup>

School of Mechanical Engineering, Sungkyunkwan University, Suwon, Kyunggi-Do, 440-746, Korea, and Department of Chemical and Biomolecular Engineering, University of Illinois, Urbana, Illinois 61801

Received: September 9, 2005; In Final Form: December 11, 2005

Dielectrophoresis has received considerable attention for separating nanotubes according to electronic types. Here we examine the effects of surface conductivity of semiconducting single walled carbon nanotubes (SWNT), induced by ionic surfactants, on the sign of dielectrophoretic force. The crossover frequency of semiconducting SWNT increases rapidly as the conductivity ratio between the particle and medium increases, leading to an incomplete separation of ionic surfactant suspended SWNT at an electric field frequency of 10 MHz. To reduce the conductivity ratio, the surface charge of SWNT is neutralized by an equimolar mixture of anionic surfactant sodium dodecyl sulfate (SDS) and cationic surfactant cetyltrimethylammonium bromide (CTAB), resulting in negative dielectrophoresis of semiconducting species at 10 MHz. A comparative Raman spectroscopy study shows a nearly complete separation of metallic SWNT.

## Introduction

Single-walled carbon nanotubes (SWNT) have considerable potential as components for future nanoscale electronic applications.<sup>1–4</sup> The main barrier to the realization of nanotube-based electronic devices is the inability to separate according to electronic structure.<sup>5–9</sup> All known synthetic techniques produce polydispersed mixtures of metallic, semimetallic and semiconducting fractions.<sup>9</sup> Recently, alternating current dielectrophoresis has attracted much attention as a possible candidate to address this hurdle,<sup>6–8,10–13</sup> combined with a surfactant-stabilized suspension method with high yields of individual SWNT.<sup>14,15</sup>

A dielectric particle dispersed in solution polarizes following the application of an electric field. The Clausius–Mossotti factor, consisting of dielectric constant, conductivity and the frequency of electric field, represents the effective polarizability of the particle.<sup>16</sup> Positive dielectrophoresis (toward the electrode) is observed for metallic SWNT due to the large dielectric constant.<sup>6,8</sup> However, it is shown that semiconducting SWNT display either positive or negative (repulsive) dielectrophoresis depending on the electric field frequency and the particle surface conductivity induced by the interaction between SWNT and the anionic surfactant.<sup>6,7,12,13</sup> The sign of the Clausius–Mossotti factor for metallic tubes can also be reversed by functionalization using diazonium reagents, due to a large decrease in conductivity and dielectric constant.<sup>6</sup>

In this paper, the induced surface conductivity effect on dielectrophoretic mobility is examined in detail using cationic/anionic surfactant mixtures. A nearly complete separation between metallic and semiconducting SWNT is demonstrated, by a comparative Raman spectroscopy study on the dielectro-

phoretically deposited tubes, when the surface charge is neutralized. A theoretical analysis also shows the change in the direction of dielectrophoretic force, depending on the surface conductivity, for semiconducting SWNT.

## Experimental Section

The electrodes with multiple gaps were fabricated using photolithography as shown in Figure 1. The distance between bases of electrodes was 25  $\mu\text{m}$ , and the gap size was 5  $\mu\text{m}$ . The 5 nm titanium and 100 nm gold contacts were sputtered on a  $\text{SiO}_2$ –Si substrate. The thickness of the  $\text{SiO}_2$  layer was 300 nm. Anionic surfactant sodium dodecyl sulfate (SDS), cationic surfactant cetyltrimethylammonium bromide (CTAB), and catanionic mixtures of SDS and CTAB were used to suspend HiPco-SWNT according to a previously published protocol that involves high-shear homogenization, ultrasonication, and ultracentrifugation.<sup>14</sup>

A drop of HiPco-SWNT (10  $\mu\text{L}$ ) was placed on the electrode after applying alternating current at a frequency of 10 MHz and a peak-to-peak voltage ( $V_{\text{p-p}}$ ) of 10 V. The alternating current was applied using a function generator (Agilent 33220A, maximum frequency = 20 MHz). The droplet was blown off using nitrogen gas after a delay of 10 min, and the electric field was turned off. The minimum electric field strength to move nanotubes by dielectrophoresis, despite the effects of Brownian motion, was determined to be on the order of 1 V/ $\mu\text{m}$ .<sup>7</sup> The electric field at the gap was 2 V/ $\mu\text{m}$ , while the intensity between bases of electrodes was 0.4 V/ $\mu\text{m}$ . The inset to Figure 1 shows dielectrophoretically deposited nanotubes at the gap. Dielectrophoretically deposited nanotubes were characterized with a Raman microscope (Renishaw, inVia Reflex) without any rinsing. A HeNe laser with a grating of 1800 grooves/mm was used for 633 nm excitation. The laser power at the sample was 20 mW, and the spot size was 1–2  $\mu\text{m}$  in diameter.

\* Corresponding author. Mailing address: 300 Chunchun-dong, Jangnan-gu, Suwon, Kyunggi-do, 440-746, Korea. Telephone: (+82)-31-290-7456. Fax: (+82)-31-290-5881. Email: sbaik@me.skku.ac.kr.

<sup>†</sup> Sungkyunkwan University.

<sup>‡</sup> University of Illinois.

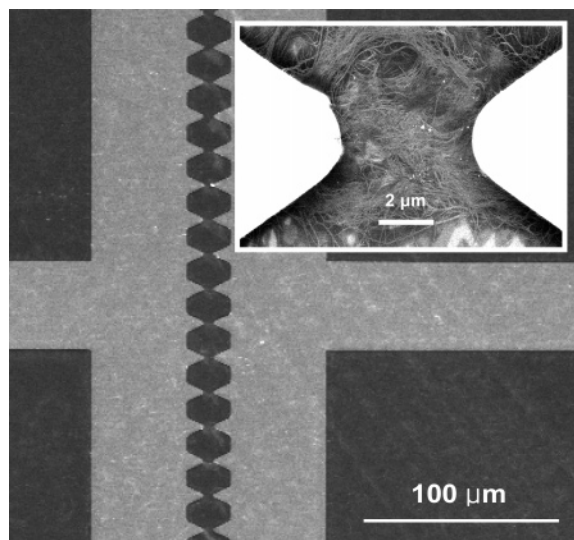


**Figure 1.** Electrode configuration used in this work. The inset shows a matted sheet of nanotubes deposited, by ac dielectrophoresis, at the 5  $\mu\text{m}$  gap.

## Results and Discussion

Figure 2a shows absorption spectra of SWNT suspended by anionic surfactant SDS (1 wt %) and cationic surfactant CTAB (1 wt %), respectively. The absorption spectrum of CTAB suspended SWNT shows broadened and red-shifted features, compared to that of SDS-suspended SWNT, which is in agreement with previous observation.<sup>15</sup> Figure 2b shows Raman results of SDS suspended SWNT. The radial breathing mode spectrum measured on dielectrophoretically deposited SWNT is compared with that of a reference sample. A drop of nanotube suspension was air-dried onto a glass slide for the reference sample, and residual surfactant was observed on the dried spot (see Supporting Information). Both the dielectrophoretically deposited material and the reference sample were characterized without any rinsing. The similarities in the change of Raman spectra are observed for CTAB suspended SWNT (Figure 2c) although the surfactant is positively charged. At 633 nm excitation, both metallic and semiconducting tubes are in resonance for the HiPco material. The apparent increase in metallic modes with small semiconducting peaks, compared to those of control samples, could be attributed to a combination of three factors.

First, semiconducting nanotubes can have positive dielectrophoresis at the electric field frequency of 10 MHz, depending on the induced surface conductance by ionic surfactants, while metallic nanotubes always experience positive dielectrophoresis. A dielectric particle in a dielectric medium experiences a force, to regions of high or low field strength, in proportion to the Clausius–Mossotti (CM) factor.<sup>16,17</sup> Equation 1 describes the CM factor derived for a long rod with its major axis parallel to an inhomogeneous alternating electric field.<sup>7,17</sup>

$$f_{\text{CM}} = \frac{\frac{\epsilon_p - \epsilon_m}{\epsilon_m + (\epsilon_p - \epsilon_m)L}}{\epsilon_m + (\epsilon_p - \epsilon_m)L} \quad (1)$$

$$\epsilon_p = \epsilon_p - i\frac{K_p}{\omega}, \quad \epsilon_m = \epsilon_m - i\frac{K_m}{\omega} \quad (2)$$

where  $\epsilon$  is the permittivity,  $K$  is the conductivity, and  $\omega$  is the frequency of the electric field. The subscripts m and p refer to the suspending medium and particle, respectively. The depo-

larization factor  $L$  is approximated by  $L = d^2/l^2[\ln(2l/d) - 1]$ .  $d$  and  $l$  denote the diameter and length of a tube. The force acts to move the particle to regions of high field strength when the sign of the real part of the Clausius–Mossotti factor is positive, and the particle moves toward regions of low field strength when the CM factor is negative. The crossover frequency is where the dielectrophoretic force is zero; i.e., the CM factor is zero. Particles experience positive dielectrophoresis at the frequencies smaller than the crossover frequency. The static dielectric constant of SWNT is inversely proportional to the square of the band gap energy.<sup>18</sup> The dielectric value of metallic SWNT should be exceedingly large, while that of semiconducting SWNT was found to be smaller than 5.<sup>8,19</sup>

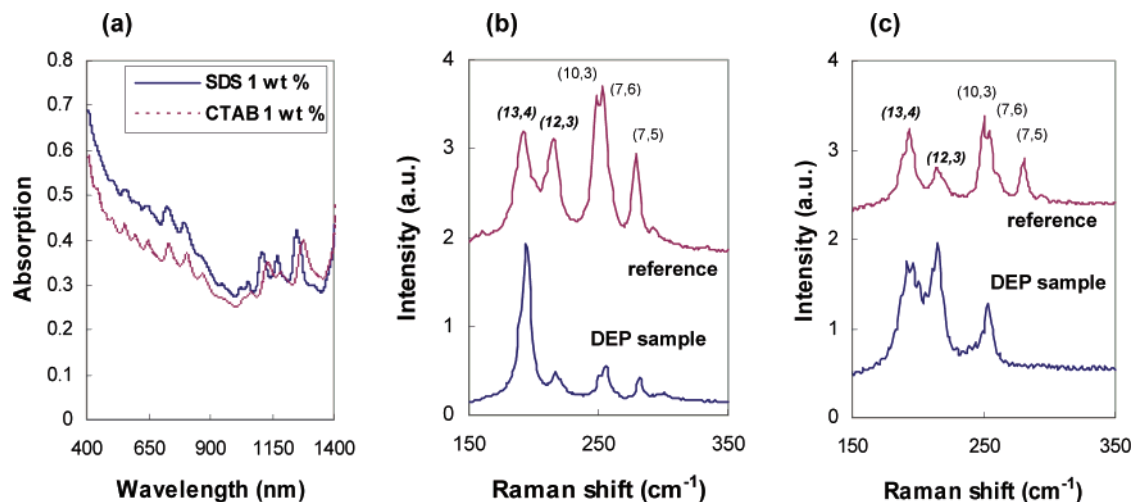
Figure 3 shows the predicted CM factor at 10 MHz as a function of two parameters:  $\alpha = \epsilon_p/\epsilon_m$  and  $\beta = K_p/K_m$ . Values of  $\epsilon_m = 80$  and  $K_m = 0.0971$  S/m, previously measured for 1% SDS/D<sub>2</sub>O,<sup>6</sup> were used for the calculation. The depolarization factor  $L$  was assumed to be  $10^{-5}$  ( $d = 1$  nm,  $l = 800$  nm). Positive dielectrophoresis is always observed for particles with large  $\alpha$  values: i.e., metallic SWNT. However, either positive or negative dielectrophoresis is predicted for semiconducting tubes, with  $\alpha$  values smaller than 0.0625, depending on the conductivity of particle with respect to that of the medium. The conductivity of a spherical in an electrolyte can be expressed as<sup>16,20</sup>

$$K_p = K_{\text{int}} + \frac{2\lambda}{a} \quad (3)$$

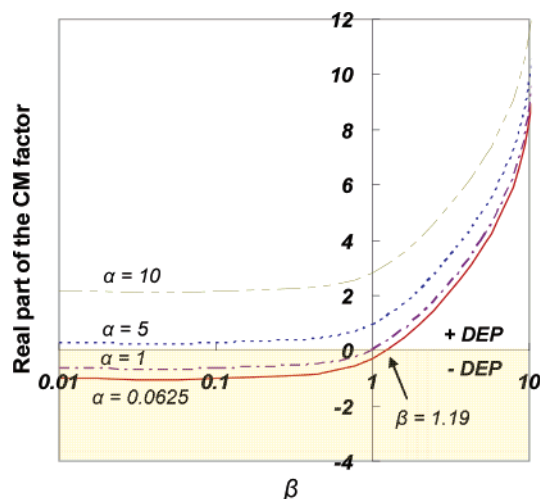
where  $K_{\text{int}}$  is the internal particle conductivity,  $\lambda$  is surface conductance and  $a$  is the radius of a spherical particle. The surface conductance component can be caused by the movement of ions, or charged surfactants, in the solution medium to the surface of the particle.<sup>6,7,16</sup> This effect can augment the conductivity by many times the intrinsic value, resulting in the change of the direction of dielectrophoretic force for semiconducting SWNT. The adsorption properties of ionic surfactants mean that more surfactant molecules are found at the interface between hydrophilic and hydrophobic phases, which gives rise to a higher surface conductance of SWNT than that of the solution medium. The relative difference in conductivity between the SWNT and medium greatly affects the sign and strength of dielectrophoretic force.

Figure 4 shows the variation in crossover frequency for semiconducting SWNT with  $\alpha = 0.0625$ . The crossover frequency is zero when  $\beta = 1$  and increases rapidly as  $\beta$  increases. The dependency of the crossover frequency on  $\alpha$  and  $\beta$  has also been described in ref 7. Figure 4 clearly shows that the crossover frequency is greater than 10 MHz when  $\beta$  is greater than 1.19. The graphs of nanotubes with smaller  $\alpha$  values almost overlapped with that of the tube with  $\alpha = 0.0625$ . The  $\beta$  value of ionic surfactant suspended SWNT is expected to be greater than 1.19, due to the adsorption properties of surfactants, resulting in positive dielectrophoresis of semiconducting SWNT at 10 MHz. As shown in Figure 3, both metallic and semiconducting SWNT have positive dielectrophoresis when  $\beta$  is greater than 1.19. However, metallic SWNT are expected to be enriched in the dielectrophoretically deposited sample since the magnitudes of the CM factors of metallic SWNT are greater than those of semiconducting types.

Second, a transition shift due to the different sample morphology (i.e., nanotube bundle status) can result in similar feature changes in the radial breathing mode spectra shown in Figure 2b, as we systematically demonstrated in refs 6 and 26 by comparing with different control samples. Recently, Ericson



**Figure 2.** (a) Absorption spectra of suspended tubes by SDS and CTAB, respectively. (b) Raman spectra of tubes deposited from the SDS suspension by air-drying onto a glass slide (reference) and by dielectrophoresis, respectively. The reference was prepared by air-drying a drop of nanotube suspension onto a glass slide. (c) Raman spectra for tubes deposited from the CTAB suspension by air-drying onto a glass slide (reference) and by dielectrophoresis.



**Figure 3.** Theoretical plot showing the variation in the real part of the Clausius–Mossotti factor as a function of two parameters,  $\alpha = \epsilon_p/\epsilon_m$  and  $\beta = K_p/K_m$ , using values of  $\epsilon_m = 80$ ,  $K_m = 0.0971$  S/m and  $L = 10^{-5}$ . The conductivity of the 1 wt % SDS/D<sub>2</sub>O solution was used for  $K_m$ .<sup>6</sup> The frequency used in the calculation was 10 MHz.

and Pehrsson also carried out a detailed study about the aggregation effects on the Raman spectroscopy of dielectrophoretically deposited SWNT, showing that aggregation plays an important role in the changes of metallic to semiconducting SWNT ratios.<sup>21</sup> This complicates the use of Raman to benchmark a potential separation, and the characterization of electronic separation in ref 8 is ambiguous because of these bundling-induced Raman changes.<sup>6,21</sup> The change in Raman spectra, due to the enrichment of specific electronic types, could be overestimated or underestimated by the different chemical/physical environments. Electrical transport measurements also confirmed the presence of both metallic and semiconducting types in the dielectrophoretically deposited, ionic surfactant-micellized SWNT.<sup>6</sup>

Finally, a small number of residual bundles can exist in the ultracentrifuged sample, as noted by other researchers,<sup>8,12,15</sup> leading to an incomplete separation. Bundles, containing semiconducting tubes and at least one metallic tube with a large dielectric constant, will move to regions of high field strength.<sup>8</sup>

Anionic SDS was added to cationic CTAB suspended SWNT solution to examine surface conductance effects on dielectro-

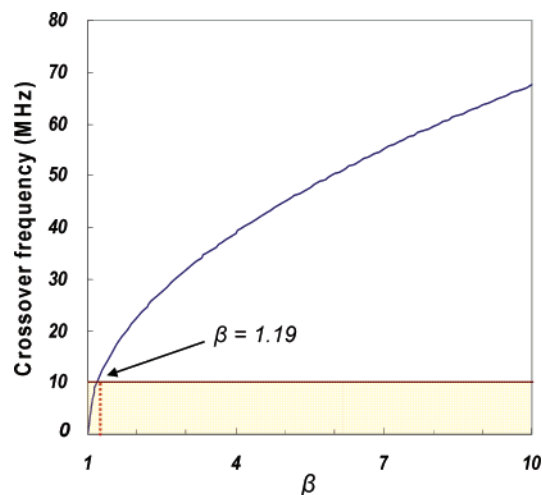


**Figure 4.** Calculated frequency at  $f_{CM} = 0$  (i.e., crossover frequency) for semiconducting SWNT,  $\alpha = 0.0625$ , is shown as a function of  $\beta$ . The values of  $\epsilon_m = 80$ ,  $K_m = 0.0971$  S/m and  $L = 10^{-5}$  were used for the calculation.

phoretic mobility experimentally. This catanionic surfactant is an amphiphilic compound that contains cations and anions, and can be considered as a zwitterionic pseudo double-chained surfactant.<sup>22–25</sup> Tamašić et al. observed the spontaneous formation of large diameter vesicles on the order of 600 nm as well as a smaller population of crystallites of surfactant on the order of 8000 nm in the equimolar mixture of SDS and CTAB due to reduced electrostatic repulsion.<sup>23</sup> The reduced electrostatic repulsion also increases packing at the hydrophilic/hydrophobic interface.<sup>23</sup> No flocculation of SWNT was observed by mixing SDS with CTAB suspended SWNT due to the increased packing at the tube surface.

Three different concentrations of SDS were added to 27.4 mM (1 wt %) CTAB suspended SWNT, resulting in molar ratios of 1:1, 1:2 and 6:1 (SDS:CTAB). Previous zeta potential measurements revealed positively charged particles in the mixtures with CTAB in excess and vice versa.<sup>23</sup> Ionic conductivity was decreased to zero at the equimolar mixture.

Figure 5 shows results of SWNT suspended with an equimolar mixture of SDS and CTAB. Figure 5a shows the radial breathing mode regions of Raman spectra for three control samples. Chiral vectors for metallic tubes are shown in bold

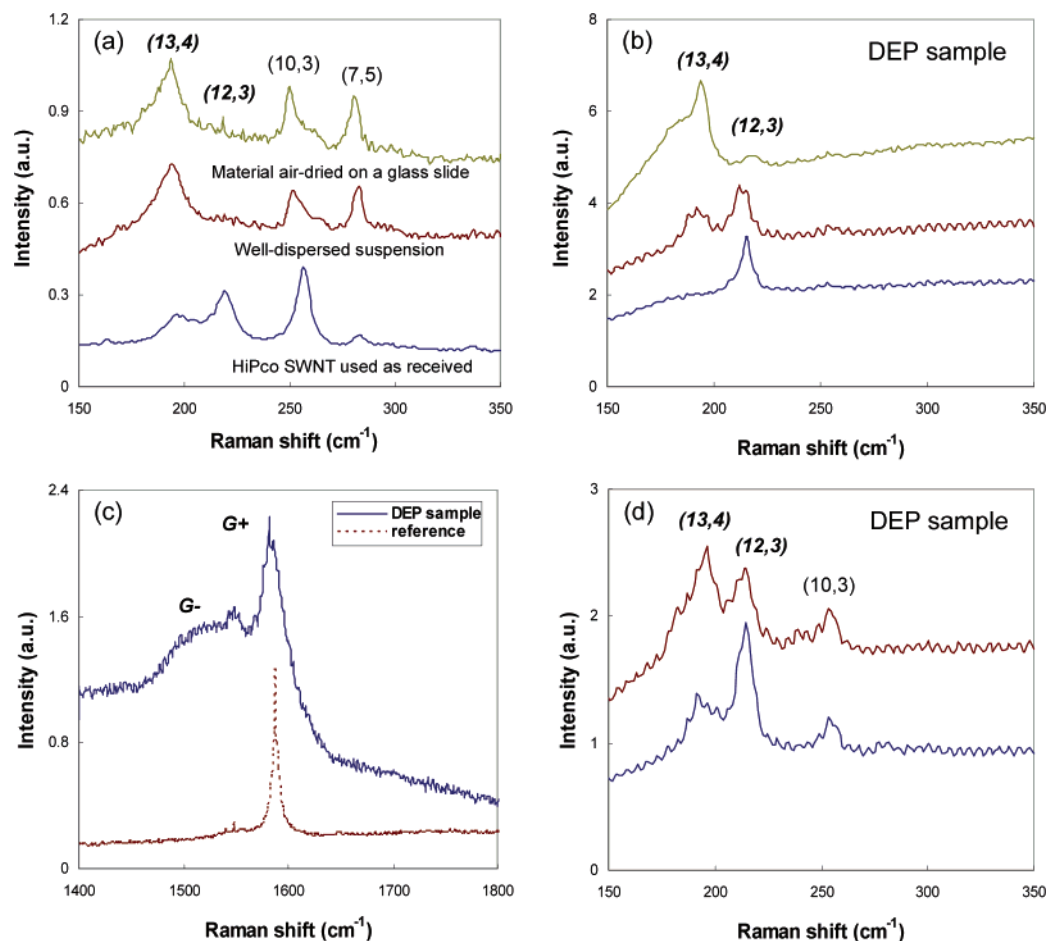


**Figure 5.** Raman spectra, at 633 nm excitation, of SWNT suspended using an equimolar mixture of SDS and CTAB (a) Radial breathing modes of three control samples; i.e., material air-dried on a glass slide, well-dispersed suspension and a deposit which was never exposed to a surfactant. (b) Radial breathing modes of dielectrophoretically deposited material. Peaks associated with semiconducting SWNT do not exist (c) G-mode region. (d) Peaks associated with metallic and semiconducting SWNT. These could be observed for dielectrophoretically deposited samples at a small number of electrode gaps.

italics. The spectrum of the air-dried material on a glass slide shows both metallic and semiconducting modes. Data from the extremes of disaggregation and bundling are also shown. Raman spectra of a well-dispersed suspension and a deposit which was never exposed to a surfactant, and is thus presumed to be completely bundled, would provide boundaries for the possible magnitude variation of the bundling effects. Different metallic to semiconducting SWNT ratios were observed for the samples at different aggregation status. However, semiconducting peaks were always present for all three control samples.

Three representative Raman spectra for dielectrophoretically deposited nanotubes are shown in Figure 5b. The peaks associated with semiconducting SWNT completely disappeared, while metallic modes are clearly shown. The relative intensities of Raman modes can change depending on the aggregation state of SWNT, which complicates the interpretation.<sup>6,21,26</sup> However, semiconducting peaks were always observed for the control samples shown in Figure 5a. Moreover, comparison of the Raman spectra of dielectrophoretically deposited, neutrally charged surfactant-micellized SWNT (Figure 5b) to those of dielectrophoretically deposited, ionic surfactant-micellized SWNT (Figure 2, parts b and c) shows a nearly complete separation of the metallic SWNT leaving the semiconducting species in the solution medium. Such dielectrophoretically deposited samples are of similar morphology. The samples shown in Figure 5b were produced above the crossover frequency, and the dielectrophoretically deposited samples shown in Figure 2, parts b

and c, were produced below the crossover frequency. As shown in Figure 5b, one metallic tube type is enriched in one case, while a different tube type is deposited preferentially in another case. This variation could be due to the nonhomogeneous deposition of metallic tubes at the Raman measurement locations since the effects from different amounts of bundling are expected to be minimal. Electrical transport measurements could not be carried out in this electrode geometry since multiple gaps of the electrode are electrically continuous.

The G-mode regions of the dielectrophoretically deposited sample show a broad  $G^-$  mode and a small  $G^+$  mode, with respect to the air-dried material on a glass slide (Figure 5c). Tangential G modes for semiconducting SWNT exhibit both  $G^-$  and  $G^+$  modes in Lorentzian line shape, with the intensity of  $G^+$  being much larger than that of  $G^-$ .<sup>8,27</sup> The  $G^-$  mode of metallic tube shows an asymmetric Breit–Wigner–Fano line shape, and the intensities of both components are of similar intensity. Comparison of the G-mode regions of both spectra also indicates the separation of metallic SWNT. We attribute the negative dielectrophoresis of semiconducting species to the neutralized surface conductance by a cationic mixture. As shown in Figures 3 and 4, the value of the real part of CM factor is negative for semiconducting SWNT ( $\alpha = 0.0625$ ) at  $\beta = 1$  and the crossover frequency is smaller than 10 MHz. As shown in Figure 5d, both metallic and semiconducting chiralities were observed for dielectrophoretically deposited samples at a small number of electrode gaps. This could be due to the



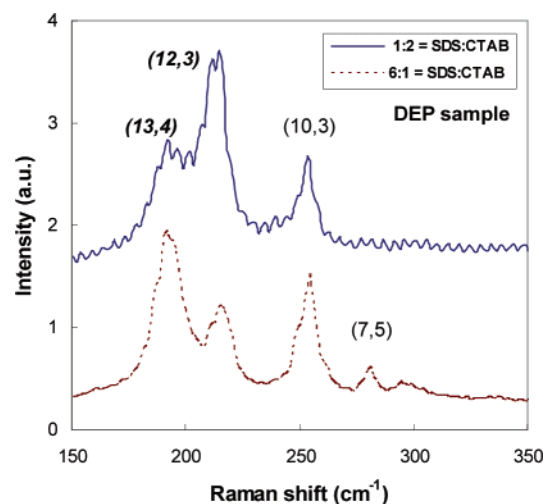


**Figure 6.** Raman spectra from tubes deposited by dielectrophoresis from suspensions of a SDS-rich (SDS:CTAB = 6:1) mixture and a CTAB-rich (SDS:CTAB = 1:2) mixture, respectively.

presence of a small concentration of bundles, containing both metallic and semiconducting species, in the solution. The aggregation status of these samples should be similar to that of samples shown in Figure 5b. Therefore, the variation in Raman spectra due to the different sample morphology should be insignificant.

Figure 6 shows Raman spectra from tubes deposited by dielectrophoresis from suspensions of a SDS-rich mixture (overall negative charge) and a CTAB-rich mixture (overall positive charge), respectively. Semiconducting SWNT have positive dielectrophoresis due to the increased surface conductance, and the radial breathing modes associated with both electronic types were observed.

## Conclusion

The theoretical and experimental results demonstrate the significant effects of surface induced conductivity, for ionic surfactant suspended semiconducting SWNT, on the sign of the dielectrophoretic force. The surface induced charge could be neutralized by an equimolar mixture of anionic SDS and cationic CTAB, resulting in negative dielectrophoresis of semiconducting SWNT at the electric field frequency of 10 MHz. Raman spectra measured on dielectrophoretically deposited nanotubes show a nearly complete separation of metallic SWNT leaving semiconducting species in the solution medium. A more detailed study to further decrease the conductivity of the nanotubes, with respect to that of the medium, should be interesting. Electrical transport measurements, with a new electrode configuration, would provide further supports for the spectroscopic observation.

**Acknowledgment.** This work was supported by Safety and Structural Integrity Research Center at Sungkyunkwan Univer-

sity and by a grant (05K1401-00410) from Center for Nanoscale Mechatronics & Manufacturing, one of the 21st Century Frontier Research Programs, which are supported by Ministry of Science and Technology, KOREA. The authors acknowledge Younghee Lee at Center for Nanotubes and Nanostructured Composites for micro-Raman measurements.

**Supporting Information Available:** A figure showing AFM and SEM images of the air-dried material (reference). This material is available free of charge via the Internet at <http://pubs.acs.org>.

## References and Notes

- (1) McEuen, P. *Phys. World* **2000**, 13, 31.
- (2) Avouris, Ph. *Acc. Chem. Res.* **2002**, 35, 1026.
- (3) Yao, Z.; Kane, C. L.; Dekker, C. *Phys. Rev. Lett.* **2000**, 84, 2941.
- (4) Tans, S. J.; Verschueren, A. R. M.; Dekker, C. *Nature* **1998**, 393, 49.
- (5) Strano, M. S.; Dyke, C. A.; Usrey, M. L.; Barone, P. W.; Allen, M. J.; Shan, H.; Kittrell, C.; Hauge, R. H.; Tour, J. M.; Smalley, R. E. *Science* **2003**, 301, 1519.
- (6) Baik, S.; Usrey, M.; Rotkina, L.; Strano, M. S. *J. Phys. Chem. B* **2004**, 108, 15560.
- (7) Krupke, R.; Hennrich, F.; Kappes, M.; Lohneysen, H. *Nano Lett.* **2004**, 4 (8), 1395–1399.
- (8) Krupke, R.; Hennrich, F.; Lohneysen, H.; Kappes, M. *Science* **2003**, 301, 344.
- (9) Dresselhaus, M. S.; Dresselhaus, G.; Avouris, Ph. *Carbon Nanotubes: Synthesis, Structure, Properties and Applications*; Springer-Verlag: New York, 2001.
- (10) Lee, S. W.; Lee, D. S.; Yu, H. Y.; Campbell, E. E. B.; Park, Y. W. *Appl. Phys. A: Mater. Sci. Process.* **2004**, 78, 283.
- (11) Nagahara, L.; Amlani, I.; Lewenstein, J.; Tsui, R. *Appl. Phys. Lett.* **2002**, 80, 3826.
- (12) Krupke, R.; Hennrich, F. *J. Phys. Chem. B* **2005**, 109, 17014–17015.
- (13) Nair, N.; Strano, M. *J. Phys. Chem. B* **2005**, 109, 17016–17018.
- (14) O'Connell, M. J.; Bachilo, S.; Huffman, C.; Moore, V. C.; Strano, M.; Haroz, E.; Rialon, K.; Boul, B.; Noon, W.; Kittrell, C.; Ma, J.; Hauge, R. H.; Weisman, R.; Smalley, R. E. *Science* **2002**, 297, 593.
- (15) Moore, V. C.; Strano, M. S.; Haroz, E. H.; Hauge, R. H.; Smalley, R. E. *Nano Lett.* **2003**, 3 (10), 1379–1382.
- (16) Green, N. G.; Morgan, H. *J. Phys. Chem. B* **1999**, 103, 41–50.
- (17) Jones, T. B. *Electromechanisms of Particles*; Cambridge University Press: Cambridge, U.K., 1995.
- (18) Benedict, L. X.; Louie, S. G.; Cohen, M. L. *Phys. Rev. B* **1995**, 52, 8541.
- (19) Pichler, T.; Knupfer, M.; Golden, M. S.; Fink, J. *Phys. Rev. Lett.* **1998**, 80, 4729.
- (20) O'Lonski, C. T. *J. Phys. Chem.* **1960**, 64, 605.
- (21) Ericson, L. M.; Pehrsson, P. E. *J. Phys. Chem. B* **2005**, 109, 20276–20280.
- (22) Wang, C.; Lucy, C. A. *Electrophoresis* **2004**, 25, 825–832.
- (23) Tamašić, V.; Štefanić, I.; Filipović-Vinceković, N. *Colloid Polym. Sci.* **1999**, 277, 153–163.
- (24) Tondre, C.; Caillet, C. *Adv. Colloid Interface Sci.* **2001**, 93, 115–134.
- (25) Marques, E. F.; Regev, O.; Khan, A.; Lindman, B. *Adv. Colloid Interface Sci.* **2003**, 100, 83–104.
- (26) Heller, D.; Barone, P. W.; Swanson, J. P.; Mayrhofer, R. M.; Strano, M. S. *J. Phys. Chem. B* **2004**, 108, 6905.
- (27) Dresselhaus, M. S.; Dresselhaus, G.; Jorio, A.; Filho, A. G. S.; Saito, R. *Carbon* **2002**, 40, 2043.